ELSEVIER

Journal of Neuroscience Methods 89 (1999) 119–127

JOURNAL OF NEUROSCIENCE METHODS

Apparatus for measuring and perturbing shoulder and elbow joint positions and torques during reaching

Stephen H. Scott *

Department of Anatomy and Cell Biology, Queen's University, Kingston, Ont. K7L 3N6, Canada

Received 31 July 1998; received in revised form 16 March 1999; accepted 20 March 1999

Abstract

Visually guided reaching movements by monkeys has become an important paradigm for examining the function of various sensory and motor areas of the brain. However, a major problem with interpreting neural discharge during this motor task has been the difficulty to quantify and manipulate the mechanics of movement. To address this problem, a new experimental facility has been developed to allow neural recordings in a monkey while it makes movements with a mechanical linkage attached to its arm. The device (KINARM) has hinge joints aligned with the monkey's shoulder and elbow and allows the monkey to make arm movements in the horizontal plane. Custom-made fibreglass braces attach the linkage to the monkey's forearm and arm. Motors attached to the mechanical linkage provide angular position of the joints and apply torques either to the shoulder or elbow, or both. The KINARM is used in concert with a computer projection system that provides virtual targets in the plane of the arm. Preliminary results illustrate the ability of a monkey to perform a variety of multi-joint motor tasks under various static and dynamic loads.

Keywords: Biomechanics; Motor coordination; Proximal arm; Reaching movements; Robotics

1. Introduction

Reaching movements provide an ideal paradigm for understanding how sensory information is converted into coordinated motor behavior. On the sensory side, movements to spatial targets require the integration of visual and proprioceptive information to select and plan the impending limb movement. On the motor side, force generated by a muscle generates motion at both spanned and non-spanned joints due to intersegmental dynamics (Hollerbach and Flash, 1982; Zajac and Gordon, 1989). This coupling between shoulder and elbow muscle activity and motion requires the CNS to carefully coordinate the motor patterns of muscles at these joints in order to smoothly move the hand in space.

Visually guided reaching movements by monkeys has become an important paradigm to study how regions of the brain, such as primary motor cortex (MI), are involved in the planning and control of voluntary movement (Kalaska and Crammond, 1992; Georgopoulos, 1995; Shen and Alexander, 1997; Zhang et al., 1997). In spite of many years of research, lively debate still remains on the most appropriate way for interpreting the discharge patterns of individual cells in MI. On the one side, many studies have illustrated that the discharge pattern of individual cells are broadly tuned to the direction of hand movement and that a population vector, constructed from the discharge patterns of a large sample of cells, tends to point in the direction of movement (Georgopoulos et al., 1988; Schwartz et al., 1988; Schwartz, 1994). The implication from these studies is that individual cells in MI may be related to higher level features of movement related to the global goal of the task such as the direction of hand movement. On the other side, the discharge of individual cells has been found to share common temporal and spatial features with the activity patterns of proximal arm muscles during reaching (Murphy et al., 1985; Miller et al., 1996; Scott, 1997) suggesting that MI may be involved in the details of motor output at the shoulder and elbow joints.

It seems surprising that such divergent frameworks for interpreting the neural representation in MI during

* Tel.: +1-613-533-2855; fax: +1-613-533-2566.
E-mail address: steve@biomed.queensu.ca (S.H. Scott)

0165-0270/99/$ - see front matter
PII: S0165-0270(99)00053-9

reaching movements are espoused in the literature. However, the ability to find neural correlates of movement to support these different views at least partially reflects the inherent coupling between different variables of movement (Mussa-Ivaldi, 1988; Scott and Kalaska, 1997). Extrinsic variables of movement, such as the kinematics of the hand, covary with intrinsic variables, such as motion of the shoulder or the activity of proximal arm muscles. As a result, neural activity related to a specific feature of movement will also covary with many other variables.

In order to dissociate the various parameters of movement, several studies have examined the response patterns of individual cells when reaching movements are performed under different mechanical loads or arm postures (Kalaska et al., 1989; Caminiti et al., 1990; Scott and Kalaska, 1997). A consistent finding from these studies is that the directional tuning of many MI cells are modified by load or posture. These results suggest that the activity of cells is not simply related to the direction of hand movement, but may be at least partially related to intrinsic features of the task, such as joint kinematics or kinetics. However, further progress on interpreting the nature of the discharge patterns of these cells based on features of motor execution are difficult in these studies because neural activity was only related to hand position or motion.

The major stumbling block for identifying the nature of the neural representation in MI during reaching is the difficulty of quantifying and manipulating the mechanics of multi-joint motion. The present article describes a new device developed specifically to address this problem called KINARM (kinesiological instrument for normal and altered reaching movements). The device uses a four-bar linkage and torque motors to record the motion of the arm in the horizontal plane and apply loads to each joint independently. While related devices have been developed to apply loads to the arm during multi-joint movements (Shadmehr and Mussa-Ivaldi, 1994; Gomi and Kawato, 1996), the loads have always been applied through the hand. A unique feature in the present system is that the loads are applied directly to the upper arm and forearm and allow the loads to be focused either at the shoulder or elbow joints, or both.

2. Methods

KINARM is an exoskeleton that attaches to the upper arm and forearm of a monkey (Fig. 1). The mechanical linkage allows the monkey to make combined flexion and extension movements of the shoulder and elbow joints to move its hand to targets in the horizontal plane. The linkage is adjustable to align its ball-bearing joints with the centers of rotation of the shoulder and elbow joints. Custom-made fibre-glass braces covered with a closed-cell foam provide an interface between the mechanical linkage and the monkey's arm and forearm.

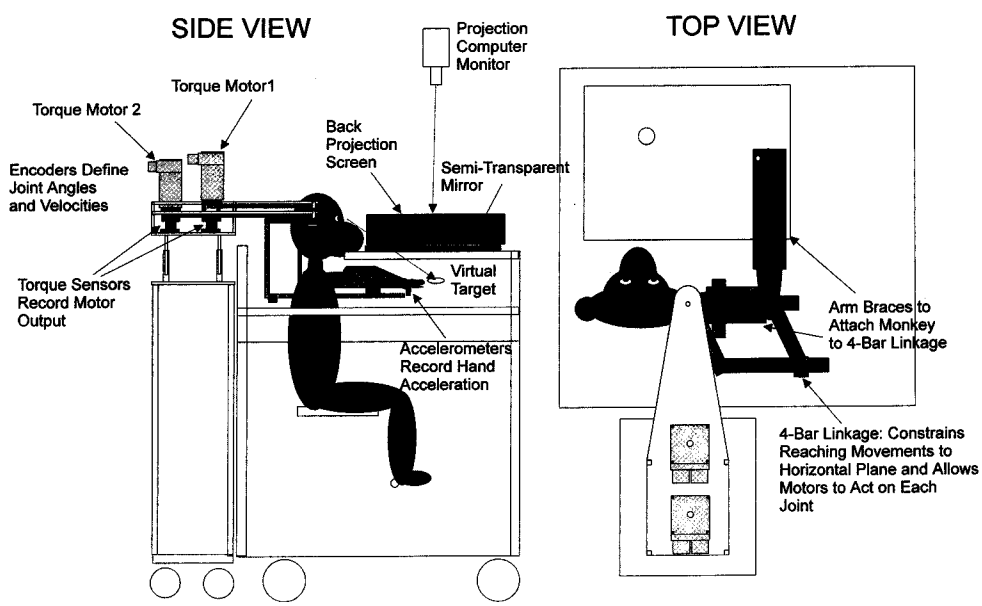

Fig. 1. (A, B) Side and top views of monkey using KINARM. Hinge joints are adjustable and can be aligned with the center of rotation of the monkey's shoulder and elbow joints. The linkage allows the monkey to move its hand in the horizontal plane by making combined flexion and extension movements at the shoulder and elbow. Each motor is attached to the device using timing belts and can modify the mechanical load at the shoulder and/or elbow joints. Accelerometers are located underneath the monkey's hand and torque sensors are attached to the base of the torque motors. A computer projection system including a semi-transparent mirror display spatial targets onto the plane of the motor task.

An important feature of KINARM is its ability to manipulate directly the mechanical characteristics of the shoulder and elbow joints using torque motors (COMPUMOTOR, SM232A motor, APEX10 motor driver, AT6450 programmable control card). Timing belts connect each motor to the mechanical linkage and allow motor 1 to act on the upper arm and motor 2 to act indirectly on the forearm. Loads at the elbow joint are applied by motor 2, whereas loads at the shoulder are applied by the combined action of motors 1 and 2.

KINARM measures several kinesiological variables of movement. Joint angular position is obtained from motor encoders with a resolution of 8192 units per revolution. Hand position is computed from the joint angles using trigonometry while hand acceleration is measured by two linear accelerometers (Entran, EGAXT-5) attached to KINARM just below the hand. The magnitude of torque applied to the mechanical linkage by each motor is monitored using reaction torque sensors (Transducer Techniques, TRT-50) attached to the base of the motors.

2.1. Equations of motion

The time-varying net muscular torque generated at the shoulder and elbow can be estimated during limb movements given the kinematics of the joints, and the length, mass and inertial characteristics of KINARM and the monkey's arm. Previous studies have documented the equations of motion for a two-joint system to describe planar limb motion (Hollerbach and Flash, 1982; Karst and Hasan, 1991). In the present situation, the equations of motion must also consider the properties of the four-bar linkage and the two torque motors. For the description of these equations, a link will signify a rigid component of KINARM, a body segment will signify the upper arm or the forearm/hand of the monkey, and a segment will signify the combined properties of a link attached to a body segment. For example, segment 1 represents the combined properties of link 1 and body segment 1.

The monkey's arm was modeled as two rigid bodies, the upper arm and the combined forearm and hand, with single degree-of-freedom joints at the shoulder and elbow. Motion of the shoulder and elbow was defined by relative angles between the two adjacent body segments (Fig. 2B). Flexor angular motion and torque are both defined as positive, whereas extensor terms are negative. To simplify the presentation of the equations, links 3 and 4 connecting motor 2 to the forearm (see Fig. 2D) are treated separately as a two-link system and described by,

$$T_{m2} = (I_{m2} + I_3 + I_4 + m_3c_3^2 + m_4(l_3^2 + c_4^2 + 2l_3c_4\cos\Theta_4))\ddot{\Theta}_3 + (I_4 + m_4c_4^2 + m_4l_3c_4\cos\Theta_4)\ddot{\Theta}_4 - (m_4l_3c_4\sin\Theta_4)\dot{\Theta}_4^2 - (2m_4l_3c_4\sin\Theta_4)\dot{\Theta}_3\dot{\Theta}_4 - (l_3\sin\Theta_3 + l_4\sin(\Theta_3+\Theta_4))f'_X + (l_3\cos\Theta_3 + l_4\cos(\Theta_3+\Theta_4))f'_Y + d_{m2}(\dot{\Theta}_3/abs(\dot{\Theta}_3)) + g_{m2}\tanh(\dot{\Theta}_3h_{m2}) \quad (1)$$

$$0 = (I_4 + m_4c_4^2 + m_4l_3c_4\cos\Theta_4)\ddot{\Theta}_3 + (I_4 + m_4c_4^2)\ddot{\Theta}_4 + (m_4l_3c_4\sin\Theta_4)\dot{\Theta}_3^2 - l_4\sin(\Theta_3+\Theta_4))f'_X + l_4\cos(\Theta_3+\Theta_4)f'_Y \quad (2)$$

The various terms are defined in Fig. 2 and in Section 5, and their values are shown in Table 1. These equations can be solved for f'_X and f'_Y, the contact force from link 5 onto link 4 of KINARM. The equations of motion for segments 1 and 2 (see Fig. 2C) can be solved using,

$$T_s = (I_{m1} + I_1 + I_2 + m_1c_1^2 + m_2(l_1^2 + c_2^2 + 2l_1c_2\cos\Theta_2))\ddot{\Theta}_1 + (I_2 + m_2c_2^2 + m_2l_1c_2\cos\Theta_2)\ddot{\Theta}_2 - (m_2l_1c_2\sin\Theta_2)\dot{\Theta}_2^2 - (2m_2l_1c_2\sin\Theta_2)\dot{\Theta}_1\dot{\Theta}_2 - (l_1\sin\Theta_1 + l_5\sin(\Theta_1+\Theta_2-\Theta_5))f_X + (l_1\cos\Theta_1 + l_5\cos(\Theta_1+\Theta_2-\Theta_5))f_Y - T_{m1} + d_{m1}(\dot{\Theta}_1/abs(\dot{\Theta}_1)) + g_{m1}\tanh(\dot{\Theta}_1h_{m1}) \quad (3)$$

$$T_e = (I_2 + m_2c_2^2 + m_2l_1c_2\cos\Theta_2)\ddot{\Theta}_1 + (I_2 + m_2c_2^2)\ddot{\Theta}_2 + (m_2l_1c_2\sin\Theta_2)\dot{\Theta}_1^2 - l_5\sin(\Theta_1+\Theta_2-\Theta_5))f_X + l_5\cos(\Theta_1+\Theta_2-\Theta_5)f_Y + d_2(\dot{\Theta}_2/abs(\dot{\Theta}_2)) \quad (4)$$

where $f_X = -f'_X$ and $f_Y = -f'_Y$.

The constants for the static and dynamic friction terms generated by the mechanical linkage and motors were defined from direct measures of motion of the mechanical linkage (without the monkey) as torque pulses were applied by the motors. The terms were identified based on the relationship between motor torque and angular motion at a joint while the other joint was fixed and unable to rotate. Least-squares regressions were used to identify the parameters for both the static and dynamic friction terms.

Eqs. (1)–(4) contain more than 40 different variables related to the morphometric properties of the monkey's arm, the mechanical linkage and the torque motors. A test was performed to validate the accuracy of these equations to characterize the mechanics of KINARM by applying 300-ms torque pulses (± 0.15 N·m) by motor 1, motor 2 or both, while monitoring the motion of the linkage when the monkey was not wearing the device. The shoulder and elbow torques were calculated from Eqs. (1)–(4) assuming the inertial properties of the monkey's upper arm and forearm were zero. Since the monkey was not attached to the linkage, the computed muscular torques should be zero. Error in the equations of motion was defined as the root mean square (rms) of the computed shoulder and elbow

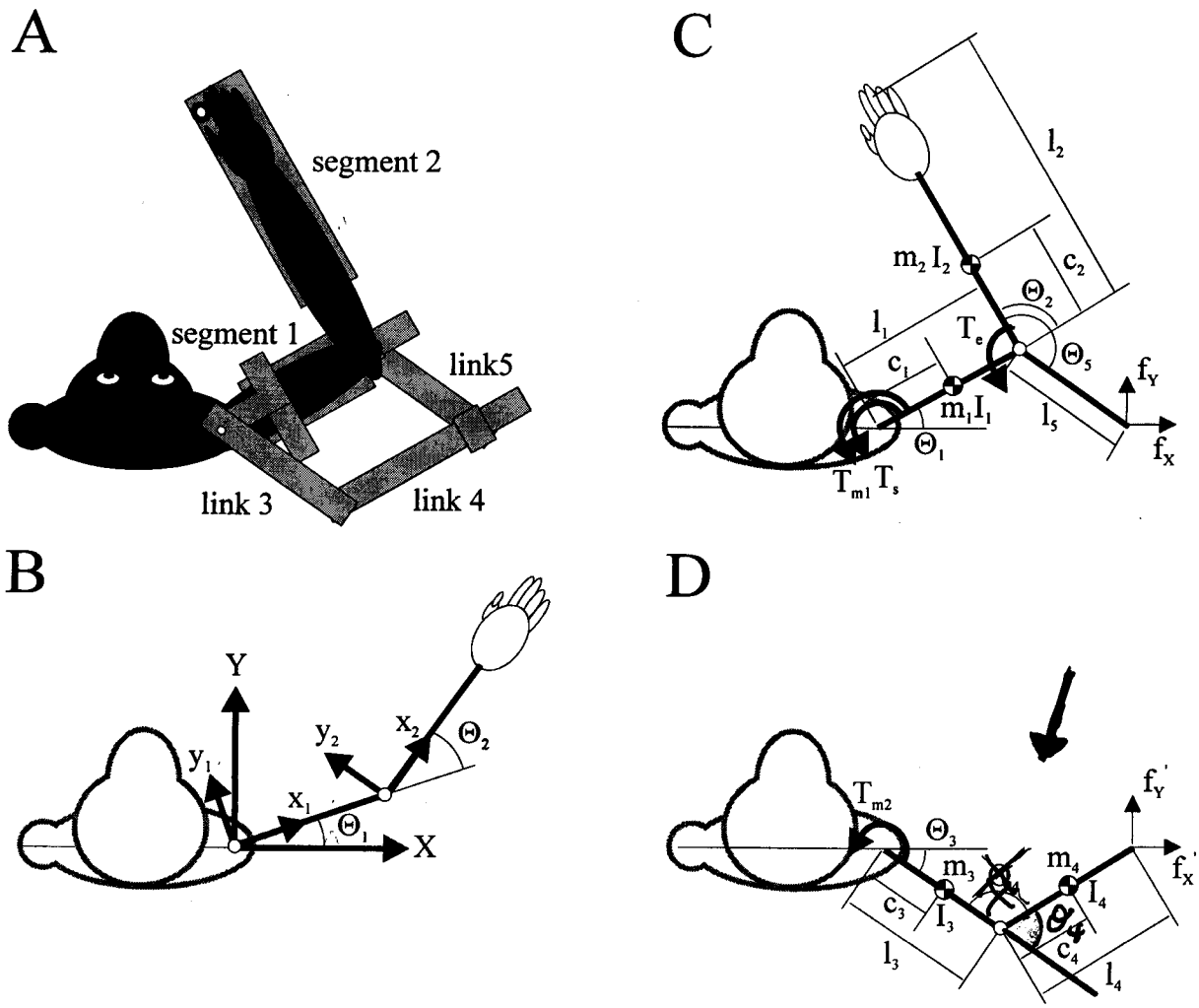

Fig. 2. (A) A simplified drawing of the monkey attached to KINARM. For descriptive purposes, a link denotes a component of KINARM, a body segment denotes a portion of the monkey, and a segment defines a body segment with an underlying link. (B) The monkey's arm is modeled as two body segments, the upper arm and the forearm/hand, with single degree-of-freedom joints at the shoulder and elbow joints. Flexor motion and torque are defined as positive (counter-clockwise), whereas extensor terms are negative (clockwise). (C) The equations of motion divide the monkey's arm and four-bar linkage into two, two-joint systems. The first two-joint system includes the arm of the monkey combined with links 1, 2 and 5. Motor 1 is attached directly to link 1. The mass and moment of inertia for segments 1 and 2 represent the combined properties for the mechanical linkage and the monkey (see Table 1). Since link 5 is rigidly attached to link 2, the angle between these two segments, Θ_5, is constant (155°). (D) The second two-joint system includes links 3 and 4 which connect motor 2 to link 5.

torques divided by the rms of the torque applied by the motors. Average error across eight torque conditions and three repetitions was 14%.

2.2. Data acquisition system

KINARM was developed in concert with a general purpose data acquisition system on a Pentium computer using LabVIEW (National Instruments). The acquisition program monitors motor encoder position, and controls the motor torque either directly or through downloadable programs to the AT6450 motor control card. Target lights, encoder position and motor commands to the motor control card are updated by the main computer approximately every 4 ms. Target information is transferred to a second computer using a serial port which displays virtual targets in the plane of the task using a semi-transparent mirror and a projection monitor (Goodbody and Wolpert, 1998; Turner et al., 1995). A data acquisition card (National Instruments, AT-MIO64E-3) provides 32 differential analog signals to monitor hand acceleration, motor torque, electromyographic activity as well as the timing of neural firing at 1000 Hz.

The analog and motor signals were analyzed using three basic procedures. First, the analog signals were low-pass filtered by removing all frequencies above 100 Hz using an FFT, then synchronized and re-sampled at 200 Hz. The signals were then filtered at 10 Hz with a low pass Butterworth Filter (Winter, 1990). The mean and standard deviation of the temporal pattern of each signal across repeated trials was determined after align-

Table 1
KINARM and monkey mechanical properties

Segment/link		l (cm)	c (cm)	m (g)	I (g·cm^2)	d (N·m)	g (N·m)	h (s/cm)
1	KINARM	12.7[c]	6.96	456	9696			
	Monkey[a]		8.62	243	2480			
	Combined		7.54	699	12 612			
2	KINARM	24.9	6.20	558	54 217	0.055		
	Monkey[a]		8.70	223	6985			
	Combined		6.90	781	62 198			
3		11.2	9.93	230	4353			
4		12.7[c]	8.13	104	3189			
5[b]		11.2						
m1					926	0.065	0.045	1.42
m2					926	0.065	0.032	1.42

[a] Monkey inertial properties scaled for juvenile male monkey (mass, 6.5 kg; arm length, 37.6 cm) from Scott (unpublished data).
[b] Link 5 is rigidly attached to link 2. Inertial parameters for link 5 are incorporated into values for link 2.
[c] The length of links 1 and 4 are adjusted to the length of the monkey's upper arm.

ing each waveform to the onset time of movement defined by the initial deviation of hand acceleration from baseline levels.

3. Results

One juvenile male monkey (6.5 kg) has been trained to wear KINARM and perform a variety of multi-joint motor tasks, including reaching movements with and without viscous loads, as well as postural tasks when intermittent or constant torque loads are applied by the device. Fig. 3 illustrates the net muscular torque at the shoulder and elbow for repeated trials in which the monkey was trained to maintain its hand at a central target while different loads were applied by the motors. A load applied at a joint requires the monkey to modify its net muscular torque (either flexion or extension) at that particular joint in order to successfully perform the task. KINARM can also apply any combination of loads at the two joints, such as a flexor load at the shoulder and an extensor load at the elbow.

Fig. 4 illustrates the kinematics and kinetics of the hand, shoulder and elbow when the monkey moved 6 cm from a central start position to a peripheral target located near its body. A shoulder extensor torque (negative) was required to initiate the limb motion followed by a small flexor torque to brake the limb motion at the spatial target. Note that while limb movement involved approximately equal motion at the shoulder and elbow joints, the magnitude of the muscular torques are much larger at the shoulder than at the elbow.

An important feature of KINARM is the ability not only to monitor the kinesiology of limb motion, but also to provide dynamic perturbations at the shoulder and/or elbow joints. A mechanical load of particular interest for movement studies are viscous loads that act only during movement. Feedback of joint angular velocity can be used to control motor torque to generate viscous loads at each joint. In this situation, the motors generate torque that opposes angular motion: the faster the movement the larger the opposing torque. The motors apply no loads when the arm is stationary. When viscous loads are initially applied by KINARM on the monkey's arm, there is a significant alteration in the arm motion including a decrease in movement speed as well as large curvatures in hand trajectory, as seen in human studies where novel loads are applied to the arm (Lackner and DiZio, 1994; Shadmehr and Mussa-Ivaldi, 1994). With considerable practise, the monkey makes roughly straight hand trajectories so that reaching movements can be performed with similar kinematic profiles, but with appreciable changes in the muscular torques at the shoulder and elbow (Fig. 5). There is a large increase in the shoulder and elbow torque for movements with viscous loads (dot-dashed)

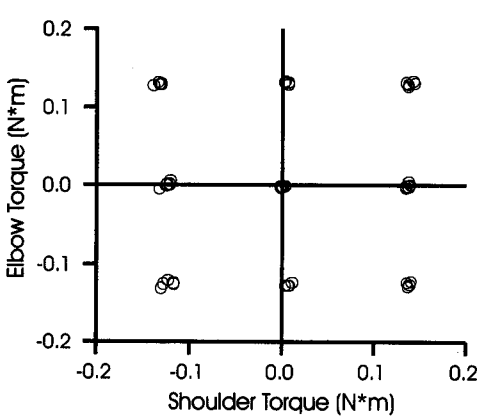

Fig. 3. The monkey was trained to maintain a similar arm posture with its hand at a central target while KINARM independently modified the load applied at each joint. Each circle denotes the net muscular torques at the shoulder and elbow for one of nine combinations of loads applied by the two torque motors (five repeat trials for each condition). Flexion torque is defined as positive.

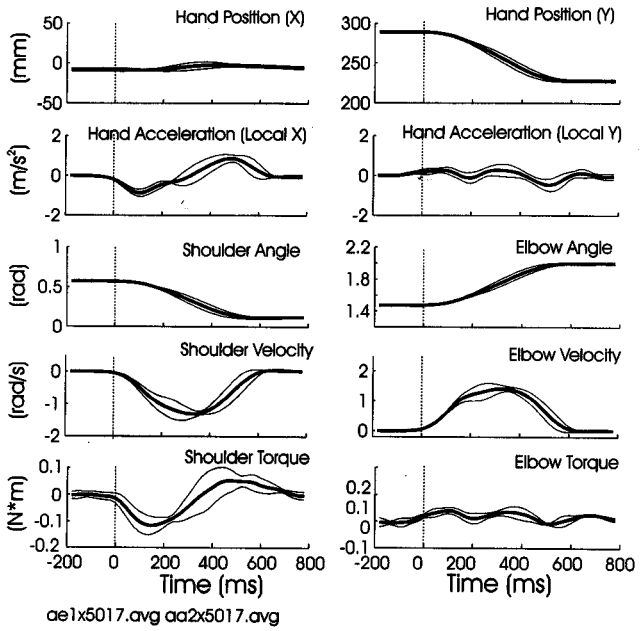

Fig. 4. The kinematics and kinetics of limb motion when the monkey made a 6-cm reaching movement from a central start position to a target located towards itself. The mean (thick line) and standard deviation (thin lines) for each variable are shown for five repeat trials. The vertical dashed line denotes the onset of movement. Flexion motion and torque are both positive.

as compared to unloaded conditions (solid). Shoulder extensor torque is increased and must be sustained for a longer time period. A braking flexor torque is not

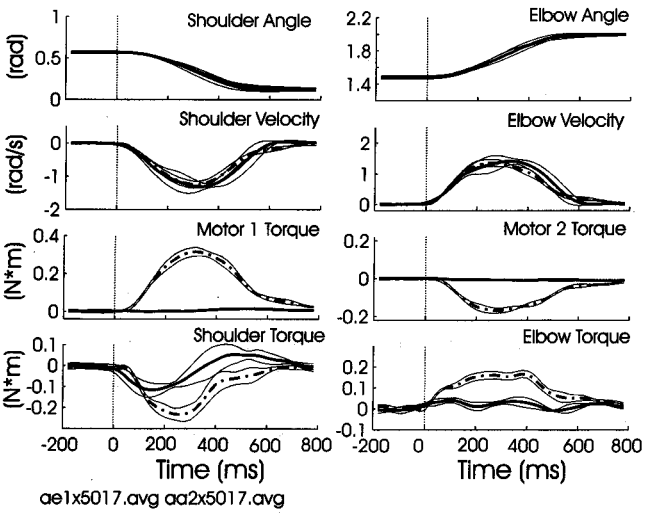

Fig. 5. Comparison of the kinematics and kinetics of limb motion with (dot-dashed line) and without (solid thick) a viscous load applied to the two joints. Thin lines denote one standard deviation for each respective signal. Movement for the unloaded condition is from Fig. 4. A viscous load is generated by the motors based on the angular velocity of the joint; the faster the motion, the larger the opposing load. Note how the joint position and velocities are quite similar for the two tasks. In contrast, there are large temporal changes in the shoulder and elbow muscular torques between viscous and unloaded conditions.

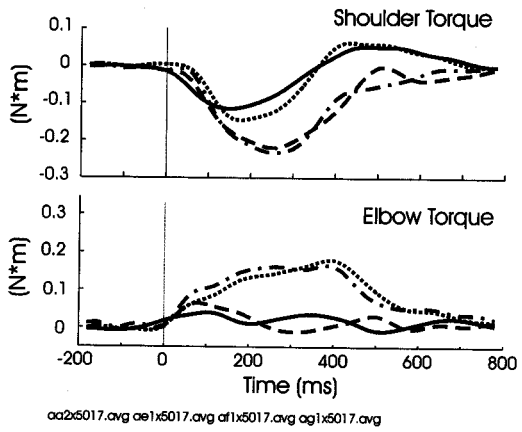

Fig. 6. KINARM allows viscous loads to be applied to each joint independently. The diagram illustrates the shoulder and elbow muscular torques from Fig. 5 where movements were performed with no loads (solid line) or with viscous loads at both joints (dot-dashed line). The diagram illustrates the mean of five repeat trials. Note that a load applied at the shoulder (dashed line) only alters the shoulder muscular torque. Viscous loads applied only at the elbow (dotted line) show a corresponding selective change in the elbow muscular torque.

required when viscous loads are added because the monkey must continue to apply an extensor torque to the end of movement to oppose the motor load. A large sustained flexor torque is required at the elbow due to the resistive force from the motors. The benefits of applying these mechanical loads during movement is that the kinetic features of movement which vary between loaded and unloaded conditions are dissociated from the kinematics of limb motion which remain constant. Moreover, KINARM allows the magnitude of the changes in joint mechanics to be quantified.

Not only can the mechanics of limb motion be altered under dynamic conditions, but the device can also selectively modify the mechanics of either the shoulder or elbow joints. Fig. 6 illustrates how the motors can be used to create specific changes in the muscular torques at either the shoulder or elbow joints during movement. The mean of the shoulder and elbow torques displayed from Fig. 5 are reproduced in Fig. 6 for movements performed without any viscous loads (solid line) and when viscous loads are added at both the shoulder and elbow joints (dot-dashed line). When a viscous load is applied only at the shoulder joint, the shoulder muscular torque pattern (dashed line) follows that observed when viscous loads were applied at both joints. In contrast, the elbow torque pattern matches that for the unloaded condition. The reverse pattern is observed when a viscous load is applied only at the elbow (dotted line); the elbow torque pattern matches the profile observed when loads were applied at both joints while the shoulder torque pattern follows that observed for unloaded movements. These results illustrate KINARM's unique ability to selectively modify

the mechanics of a single joint during a multi-joint motor task.

Another application of KINARM is to examine the functional properties of the various spinal and supraspinal reflex systems by applying transient perturbations to the limb of the monkey during static and dynamic tasks. The kinematics of limb motion can be recorded when transient loads are applied by the two torque motors (Fig. 7). Both the magnitude and time period for the applied loads can be controlled to monitor either small transient or longer sustained perturbations. Note that loads applied at either the shoulder or elbow joints will generate motion at both joints due to intersegmental interactions. In fact, it is difficult to create an unexpected perturbation that generates motion at a single joint due to the complex changes in muscular force during this paradigm.

4. Discussion

Visually guided reaching movements have become an important paradigm for studying how regions of the brain, such as primary motor cortex, are involved in planning and controlling movement (Kalaska and Crammond, 1992; Georgopoulos, 1995). These multi-joint tasks require visual information to be converted into motor patterns at the shoulder and elbow joints to move the hand through space. Due to the difficulties of monitoring the kinematics of multi-joint motion, a common approach for interpreting neural activity in areas such as primary motor cortex has been to relate the activity of neurons to the direction of hand movement. While simplifying the collection of experimental data, this approach precludes direct comparisons between neural activity and features of motor execution at the proximal arm joints.

The device presented in this article provides a number of important features to aid in quantifying and manipulating the mechanics of multi-joint movements. First, the various sensors on KINARM measure a wide range of kinematic and kinetic features related to the shoulder, elbow and hand that allow one to define coordinated limb movement at many different levels. Second, the device provides a unique way of manipulating the mechanical conditions of each joint independently since the mechanical loads are applied by an exoskeleton directly to the arm and forearm. Finally, the ability to manipulate visual and proprioceptive information on limb position using KINARM and the virtual projection system may also prove valuable for looking at neural computations related to sensorimotor integration, body position sense and kinesthesia. The facility is presently being used to study the activity of proximal arm muscles of monkeys during reaching under different loads (Cisek and Scott, 1998), as well as to record the discharge patterns of motor cortical cells.

The shoulder and elbow joints normally provide multiple degrees-of-freedom (flexion/extension, abduction/adduction and internal/external rotation at the shoulder

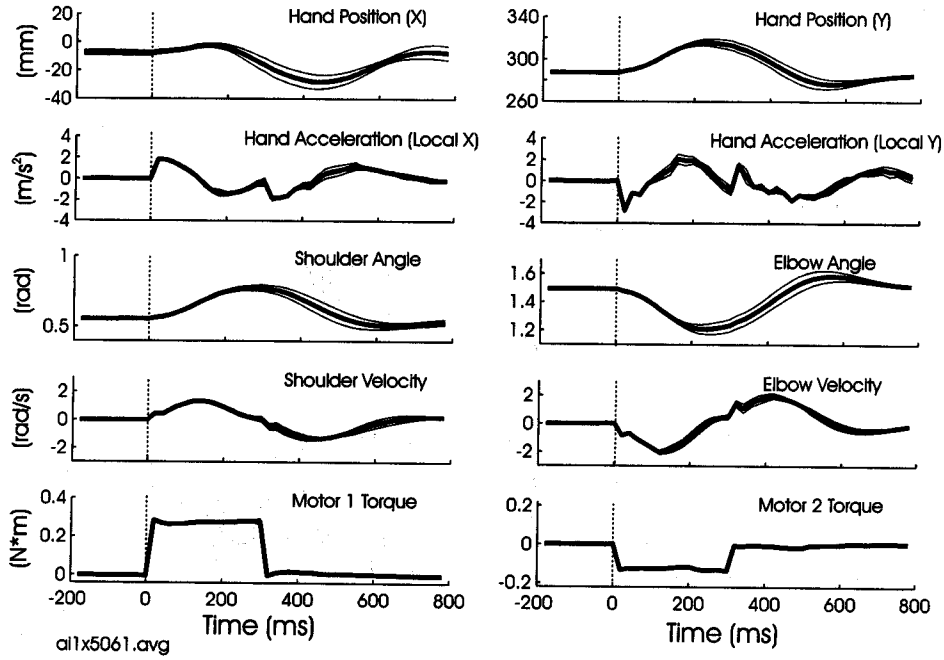

Fig. 7. The kinematics of the monkey's hand, shoulder and elbow when transient torque pulses are applied by the motors (bottom traces). The mean and standard deviation are shown for five repeat trials. The vertical line denotes the start of the torque pulse. The small inflections in the shoulder and elbow velocities at the beginning and end of the torque pulse largely reflect movement between the monkey's arm and the mechanical device due to compression of the soft tissue of the arm.

and flexion/extension and supination/pronation at the elbow) and the present device constrains motion to a single axis at each joint. The simplification was necessary to allow the mechanics of motion to be monitored easily and to allow mechanical loads to be applied to each joint. While this constraint on limb motion precludes studies on postural redundancy (e.g. Scott and Kalaska, 1997), the present system can address a wide range of issues related to multi-joint coordination, such as studies on intersegmental dynamics and control, limb trajectory redundancy, motor learning and the integration of visual and proprioceptive information to select and guide movement.

KINARM may also be valuable for studying human movement, particularly related to motor disorders. Present diagnostic and clinical assessment of multi-joint motor skills rely predominantly on qualitative descriptions of movement, such as visually verifying whether a subject can repeatedly touch their finger to their nose (O'Sullivan and Schmitz, 1994; Van Deusen and Brunt, 1997). These assessments provide only a course, subjective measure of motor function. Moreover, they provide no information on the ability of a subject to adapt their motor patterns to changes in mechanical loads, necessary for normal motor function. The range of kinesiological information provided by KINARM during multi-joint motor tasks under various mechanical conditions could be valuable as a diagnostic and motor assessment tool to identify and quantify motor dysfunction and for rehabilitation to improve motor coordination.

5. Nomenclature

c	distance from center of mass to proximal end of segment/link
d, g, h	static and dynamic friction constants
f	contact force on link 5
f'	contact force on link 4
I	moment of inertia
l	length of a segment/link
m	mass of a segment/link
T	Torque
$\Theta, \dot{\Theta}, \ddot{\Theta}$	Angular position, velocity and acceleration

Subscripts

1–5	segment/links 1–5
e	elbow joint of monkey
s	shoulder joint of monkey
m1	motor 1
m2	motor 2
x, y	cartesian coordinates (local)
X, Y	cartesian coordinates (global)

Acknowledgements

The author would like to thank a number of people that facilitated the completion of this facility; Gaetan Richard and Jacques Berichon at the Université de Montréal for drafting and machining the mechanical device, Paul Cisek for the development of software to display the kinematics and kinetics of movement, Kim Moore and Marie-Josiée Bourque for expert technical support, and Jerry Loeb and the BMEU at Queen's University for the fibre-glass arm braces and various electronic components for data acquisition. The author would also like to acknowledge financial support from the Medical Research Council of Canada (grant MT-13462). The author was supported by a FRSQ scholarship and is presently supported by an MRC Scholarship.

References

Caminiti R, Johnson PB, Urbano A. Making arm movements within different parts of space: dynamic aspects in the primate motor cortex. J Neurosci 1990;10:2039–58.

Cisek P, Scott SH. Cooperative action for mono- and bi-articular arm muscles during multi-joint posture and movement tasks in monkeys. Soc Neurosci Abstr 1998;24:164.4.

Georgopoulos AP. Current issues in directional motor control. Trends Neurosci 1995;18:506–10 (Review).

Georgopoulos AP, Kettner RE, Schwartz AB. Primate motor cortex and free arm movements to visual targets in three-dimensional space. II. Coding of the direction of movement by a neuronal population. J Neurosci 1988;8:2928–37.

Gomi H, Kawato M. Equilibrium-point control hypothesis examined by measured arm stiffness during multijoint movement. Science 1996;272:117–20.

Goodbody SJ, Wolpert DM. Temporal and amplitude generalization in motor learning. J Neurophysiol 1998;79:1825–38.

Hollerbach JM, Flash T. Dynamic interactions between limb segments during planar arm movement. Biol Cybern 1982;44:67–77.

Kalaska JF, Crammond DJ. Cerebral cortical mechanisms of reaching movements. Science 1992;255:1517–23 (Review).

Kalaska JF, Cohen DA, Hyde ML, Prud'homme M. A comparison of movement direction-related versus load direction-related activity in primate motor cortex, using a two-dimensional reaching task. J Neurosci 1989;9:2080–102.

Karst GM, Hasan Z. Timing and magnitude of electromyographic activity for two-joint arm movements in different directions. J Neurophysiol 1991;66:1594–604.

Lackner JR, DiZio P. Rapid adaptation to coriolis force perturbations of arm trajectory. J Neurophysiol 1994;72:299–313.

Miller LE, Nocher JD, Lee JS, Garg R. A muscle-space description of motor cortical discharge. Soc Neurosci Abstr 1996;22:795.7.

Murphy JT, Wong YC, Kwan HC. Sequential activation of neurons in primate motor cortex during unrestrained forelimb movement. J Neurophysiol 1985;53:435–45.

Mussa-Ivaldi FA. Do neurons in the motor cortex encode movement direction? An alternative hypothesis. Neurosci Lett 1988;91:106–11.

O'Sullivan SB, Schmitz TJ. Physical Rehabilitation: Assessment and Treatment, 3rd ed. Philadelphia, PA: Davis, 1994.

Schwartz AB. Direct cortical representation of drawing. Science 1994;265:540–2.

Schwartz AB, Kettner RE, Georgopoulos AP. Primate motor cortex and free arm movements to visual targets in three-dimensional space. i. relations between single cell discharge and direction of movement. J Neurosci 1988;8:2913–27.

Scott SH. Comparison of onset time and magnitude of activity for proximal arm muscles and motor cortical cells prior to reaching movements. J Neurophysiol 1997;77:1016–22.

Scott SH, Kalaska JF. Reaching movements with similar hand paths but different arm orientations: I. Activity of individual cells in motor cortex. J Neurophysiol 1997;77:826–52.

Shadmehr R, Mussa-Ivaldi FA. Adaptive representation of dynamics during learning of a motor task. J Neurosci 1994;14:3208–24.

Shen L, Alexander GE. Neural correlates of a spatial sensory-to-motor transformation in primary motor cortex. J Neurophysiol 1997;77:1171–94.

Turner RS, Owens JW Jr., Anderson ME. Directional variation of spatial and temporal characteristics of limb movements made by monkeys in a two-dimensional work space. J Neurophysiol 1995;74:684–97.

Van Deusen J, Brunt D. Assessment in Occupational Therapy and Physical Therapy. Philadelphia, PA: Saunders, 1997.

Winter DA. Biomechanics and Motor Control of Human Movement, 2nd ed. New York: Wiley, 1990.

Zajac FE, Gordon ME. Determining muscle's force and action in multi-articular movement. In: Pandolf KB, editor. Exercise and Sport Sciences Reviews. Baltimore: Williams & Wilkins, 1989:187–230.

Zhang J, Riehle A, Requin J, Kornblum S. Dynamics of single neuron activity in monkey primary motor cortex related to sensorimotor transformation. J Neurosci 1997;17:2227–46.